JOC The Journal of Organic Chemistry

ARTICLE

pubs.acs.org/joc

Duplex and Triplex Formation of Mixed Pyrimidine Oligonucleotides with Stacking of Phenyl-triazole Moieties in the Major Groove

Nicolai Krog Andersen,[†] Holger Døssing,[‡] Frank Jensen,[§] Birte Vester,[‡] and Poul Nielsen[†,*]

[†]Nucleic Acid Center, Department of Physics and Chemistry and [‡]Department of Biochemistry and Molecular Biology, University of Southern Denmark, 5230 Odense M, Denmark

[§]Department of Chemistry, Århus University, Langelandsgade, 8000 Århus, Denmark

Supporting Information

ABSTRACT: 5-(1-Phenyl-1,2,3-triazol-4-yl)-2′-deoxycytidine was synthesized from a modified CuAAC protocol and incorporated into mixed pyrimidine oligonucleotide sequences together with the corresponding 5-(1-phenyl-1,2,3-triazol-4-yl)-2′-deoxyuridine. With consecutive incorporations of the two modified nucleosides, improved duplex formation with a complementary RNA and improved triplex formation with a complementary DNA duplex were observed. The improvement is due to $\pi-\pi$ stacking of the phenyl-triazole moieties in the major groove. The strongest stacking and most pronounced positive influence on thermal stability was found in between the uridine analogues or with the cytidine analogue placed in the 3′ direction to the uridine analogue. Modeling indicated a different orientation of the phenyl-triazole moieties in the major groove to account for the difference between the two nucleotides. The modified oligonucleotides were all found to be significantly stabilized toward nucleolytic degration.

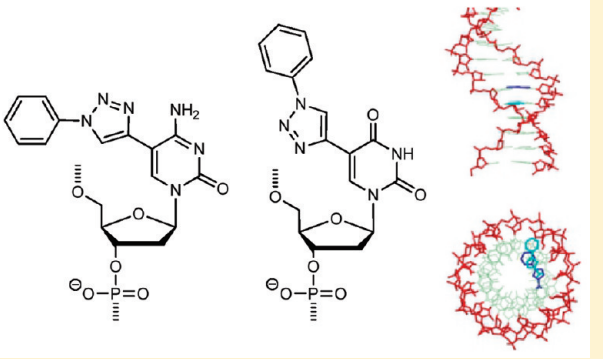

INTRODUCTION

The idea of regulating gene expression by chemically modified oligonucleotides has been pursued for three decades.[1,2] The therapeutic potential has been formulated in the so-called antisense[2,3] and antigene strategies,[4] where the molecular target is RNA and genomic double stranded DNA, respectively. The chemically modified oligonucleotides should be physiologically stable and form thermally strong duplexes with RNA or triplexes with DNA.[3,4] A significant amount of chemical modifications have been presented,[5] and among the most successful are 2′-modified nucleotides, conformationally restricted carbohydrate moieties, as in LNA,[6] and base-modified analogues.[7] As a prime example of the latter, nucleobases with extended ring systems have been found to give very strong duplexes due to increased $\pi-\pi$ stacking. Especially the phenoxazine replacement of the cytosine is a good example[8] leading to an increase in thermal stability of a DNA:RNA duplex with up to 5 °C for one incorporation, but also 5-modified (for instance 5-propynyl-) pyrimidine nucleosides have been shown to increase the duplex stability.[9] Recently, we demonstrated that simple substituted triazoles introduced in the 5-position of 2′-deoxyuridine lead to increased melting temperatures of DNA:RNA duplexes.[10] These nucleosides (like **1**, Figure 1) are easily obtained by using the CuAAC (Cu-catalyzed alkyn-azide cycloaddition) reaction[11] and can be introduced into oligonucleotides after making the appropriate phosphoramidite building block in only four synthetic steps.[10] The most pronounced results were obtained with a phenyl-substituent (**1**, R = H) and hereby a large continuous π-system. Two consecutive incorporations of **1** into the oligonucleotide were necessary to give the positive effect, which increased even further with three or four consecutive incorporations proving that $\pi-\pi$ stacking of the aromatic substituents is driving the increase in duplex stability.[10,12] Similar or slightly increased melting temperatures were obtained by the more hydrophilic phenol or benzensulfonamide substituents (**1**, R = OH or SO_2NH_2).[12] The most important limitation to the concept of obtaining improved RNA recognition by the simple stacking building block **1** is the sequence context demanding a stretch of at least two 2′-deoxyuridine derivatives in the antisense oligonucleotide. Herein we meet this challenge by the introduction of the cytidine derivative **2** (Figure 1).[13,14] This nucleoside building block can be expected to show a different conformational behavior, and therefore modeling is applied in order to understand the sequence specific behavior of stacking between **1** and **2**. Furthermore, the potential of **1** and **2** in triplex-forming oligonucleotides, as well as the stability of the oligonucleotides toward nucleolytic degradation, are investigated.

RESULTS

Modeling of the Triazole−Cytosine Bond. In our former study, ab initio calculations on a simple model compound

Received: May 9, 2011
Published: June 21, 2011

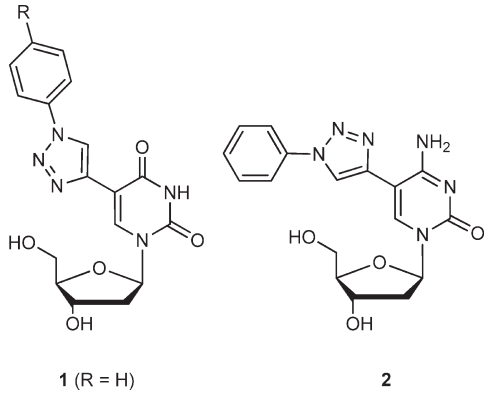

Figure 1. 5-(Phenyltriazole)pyrimidine nucleosides **1** and **2** (sketched in their preferred conformations).

(1,3-dimethyl-5-(1-methyl-1,2,3-triazole-4-yl)uracil) showed a strong preference for a coplanar organization of the triazole-uracil in **1** with the triazole-CH pointing toward O4 of the uracil (Figure 1) probably through a CH−O hydrogen bonding interaction and an N/O lone pair repulsion.[10] We rationalized, however, that this conformation might be unlikely for **2** and that the triazole might induce a different tautomeric preference for **2** as compared to natural cytitidine analogues. Therefore, a similar series of ab initio calculations and subsequent conformational analysis was performed on three tautomers of a simple dimethylated 5-(1,2,3-triazole-4-yl)cytosine derivative (Figure 2). The torsional energy profiles were obtained by single point MP2/aug-cc-pVDZ energies on MP2/6-31G(d,p) geometry relaxed scans[15] as a function of the angle ω. The profiles are shown in Figure 2 and show that the tautomer A is lower in minimal energy than tautomer B and C with 19 and 12 kJ/mol, respectively. Tautomer C is similar to the corresponding uracil analogue, and the rotational profile is almost identical to the one found for trimethylated 5-(1,2,3-triazole-4-yl)uracil[10] with a deep global minimum at 180° corresponding to the anti conformation shown for **1** in Figure 1. The reason is probably repulsion between the nitrogen lone pairs possibly in combination with a CH−N hydrogen bond interaction. The tautomers A and B display similarly shaped rotational profiles, with tautomer B being 19 kJ/mol higher in energy than A. The global minimum for tautomer B is a nonplanar anti conformation with $\omega \approx 150°$, whereas A has a broad global minimum at $\omega = 0°$ (essentially flat energy surface −30° to 30°) corresponding to the conformation drawn for **2** in Figure 1. This is probably stabilized by an internal (triazole) N−HN (cytosine) hydrogen bond. A nonplanar anti conformation with $\omega \approx 150°$ is a local minimum. These results strongly indicate that the cytidine analogue **2** will prefer the opposite coplanar conformation as compared to the uridine analogue **1** (Figure 1). This will position the phenyl group of **2** as compared to **1** with a different orientation in the major groove. A recent X-ray crystal study on **2** by Hudson and co-workers also revealed the same nearly coplanar conformation.[14]

Chemical Synthesis. The synthesis of the cytosine derivative **2** was naturally inspired by the convenient synthesis of **1**.[10] However, a protection of the exocyclic amine was necessary. After several strategies had been considered and approached,[13] we succeeded in synthesizing the 4-*N*-acetylated phosphoramidite in a series of reactions starting from 5-iodo-2′-deoxycytidine followed by a Sonogashira coupling, cycloaddition, 4-*N*-protection, 5′-*O*-tritylation, and 3′-*O*-phosphitylation (Scheme 1). Hence, the known 5-ethynyl-2′-deoxycytidine, **4**,[14,16] was made by a slightly modified procedure using an efficient Sonogashira reaction on unprotected 5-iodo-2′-deoxycytidine, **3**, and then reacted in our formerly published in situ azidation/CuAAC protocol,[10] affording 5-(4-phenyl-1,2,3-triazol-1-yl)-2′-deoxycytidine, **2**, in a good yield. Peracetylation and subsequent selective hydrolysis of the acetyl esters afforded the 4-*N*-acetylated derivative **5**. Protection of the 5′-*O*-position with the DMT (4,4′-dimethoxytrityl) group gave compound **6**, and subsequent phosphitylation afforded the phosphoramidite **7**, which can be used in standard automated solid-phase oligonucleotide synthesis.

The phosphoramidite **7** was incorporated in a series of oligonucleotide sequences in combination with the corresponding

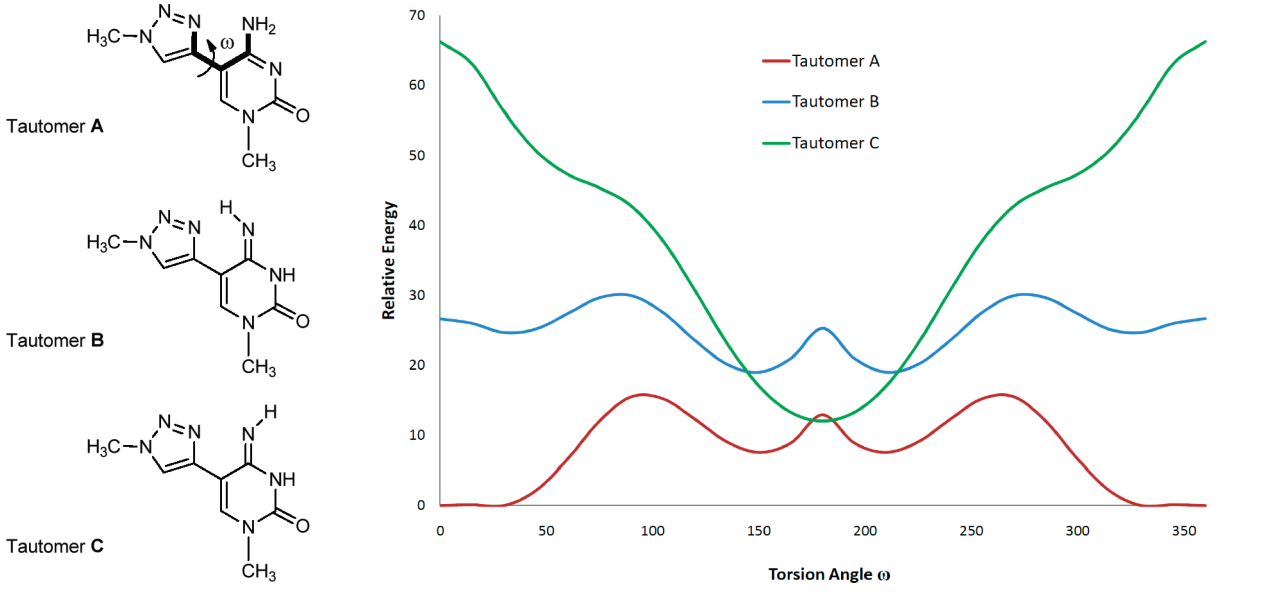

Figure 2. Ab initio calculations of rotational profiles for three tautomers of a model compound of **2**. Left, the tautomers with the definition on the torsional angle ω. The structures drawn corresponds to $\omega = 0°$. Right, torsional rotation profile for each tautomer.

dx.doi.org/10.1021/jo200919y |*J. Org. Chem.* 2011, 76, 6177–6187

phosphoramidite of **1**[10] and unmodified 2′-deoxynucleotide phosphoramidites (Table 1). The standard sequence chosen for the present study was a 16-mer mixed pyrimidine sequence, which has been previously studied as a triplex-forming oligonucleotide (TFO).[17] A pyrimidine sequence was preferred in order to allow for a range of combinations of **1** and **2**, and we expect this sequence to give a representative picture of the full sequence potential of these modifications. Hence, the modified phosphoramidites were introduced in 7 modified oligonucleotides combining 1−4 consecutive incorporations of **1** and **2** in different combinations in order to study the effect of stacking in different sequence contexts in duplexes formed with complementary DNA and RNA as well as in triplexes formed with a double stranded DNA-target.

Scheme 1[a]

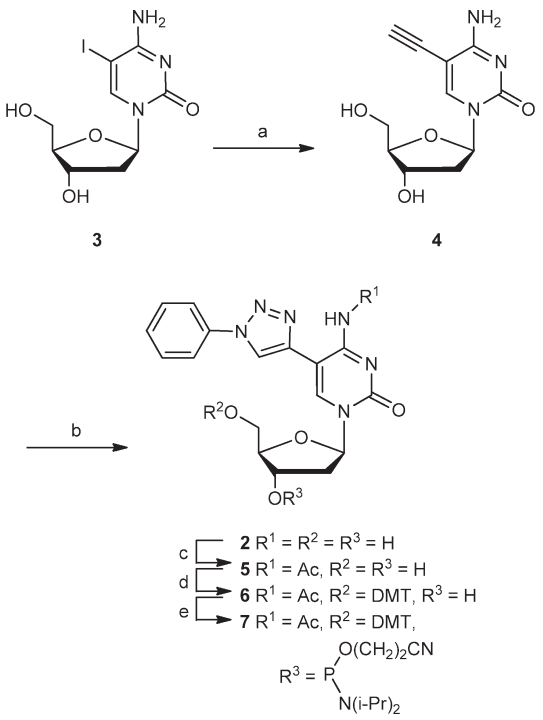

[a] Reagents and conditions: (a) (i) TMS-C≡CH, $Pd(PPh_3)_2Cl_2$, CuI, Et_3N, DMF; (ii) NH_3 (aq), 95%. (b) (i) PhBr, NaN_3, *N*,*N*-dimethylethylenediamine, CuI, EtOH/H_2O, MW 100°C; (ii) **3**, TBTA, CuI, Na ascorbate, 80%. (c) (i) Ac_2O, pyridine; (ii) 2 M NaOH, 1,4-dioxane/H_2O, 47%. (d) DMT-Cl, pyridine, 67%. (e) Diisopropylammonium tetrazolide, $NC(CH_2)_2OP(N(i\text{-}Pr)_2)_2$, $(ClCH_2)_2$, 85%. TBTA = tris-((1-benzyl-1,2,3-triazol-4-yl)methyl)amine.

Hybridization Studies. The modified oligonucleotide sequences of the present study, **ON2**−**8**, represent a series of replacements of T and dC moieties in the corresponding unmodified sequence, **ON1**, with the modified nucleosides **1** and **2** (represented as the monomers **X** and **Y**, respectively, Table 1). **ON2** and **ON3** contain single incorporations of either **1** or **2**, whereas **ON4**−**6** contains mixed consecutive incorporations of **1** or **2** and **ON7**−**8** four consecutive incorporations of either **1** or **2**, respectively. All of these ONs were mixed with complementary DNA and RNA as well as with a DNA duplex, and the melting temperatures of the duplexes or triplexes formed were determined by UV melting experiments (Table 1).

When mixed with complementary DNA, the single modified **ON2** displayed a T_m that is decreased by 1.3 °C. This is coherent with the larger decreases in T_m (3−5 °C) observed with single incorporations of **1** centrally in a shorter 9-mer sequence (the underlined positions of 5′-dGTG TTT TGC).[10,12] It can be expected that a single modification has a larger relative impact on stability in a shorter sequence. With the single incorporation of the cytidine analogue **2** in **ON3**, a slightly larger decrease in T_m with complementary DNA (ΔT_m = −1.9 °C) was observed. With a consecutive introduction of **1** and **2** in **ON4** and **ON5**, only slightly smaller decreases per modification were seen (ΔT_m = −0.6 and −1.3 °C). This is consistent with our former study of two consecutive incorporations of **1** in a 9-mer sequence (ΔT_m = −1.5 °C).[12] On the other hand, the three consecutive mixed stacking moieties in **ON6** lead to an increase in duplex stability (ΔT_m = +1.6 °C), which is in contrast to a destabilization by three consecutive incorporations of **1** in a 9-mer (ΔT_m = −1.0 °C).[12] The four incorporations of **1** (**ON7**) or of **2** (**ON8**) both display a smaller increase in duplex stability (ΔT_m = +0.6 and +0.8 °C), which corresponds well to our former study of four incorporations of **1** in a shorter 9-mer sequence (ΔT_m = −0.3 °C).[10] In general, the effects of introducing **1** and **2** in DNA:DNA duplexes are small

Table 1. Thermal stability data of modified duplexes and triplexes

	ON sequences[a]	complementary DNA[b] $T_m(\Delta T_m$/mod), °C[d]	complementary RNA[c] $T_m(\Delta T_m$/mod), °C[d]	complementary DNA duplex[e] $T_m(\Delta T_m$/mod), °C[f]
ON1	5′-dTTT TCT TTT CCC CCC T	51.9	62.7	28.0
ON2	5′-dTTT TCT TT**X** CCC CCC T	50.6 (−1.3)	64.5 (+1.8)	26.1 (−1.9)
ON3	5′-dTTT TCT TTT **Y**CC CCC T	50.0 (−1.9)	60.2 (−2.5)	23.9 (−4.1)
ON4	5′-dTTT T**YX** TTT CCC CCC T	50.8 (−0.6)	66.7 (+2.0)	24.8 (−1.6)
ON5	5′-dTTT **XY**T TTT CCC CCC T	49.4 (−1.3)	68.7 (+3.0)	25.7 (−1.2)
ON6	5′-dTTT **XYX** TTT CCC CCC T	55.0 (+1.6)	70.9 (+2.7)	30.1 (+0.7)
ON7	5′-dTTT TC**X XXX** CCC CCC T	55.0 (+0.8)	76.0 (+3.3)	35.5 (+1.9)
ON8	5′-dTTT TCT TTT **YYY** YCC T	54.3 (+0.6)	67.6 (+1.2)	nt[g]

[a] Oligodeoxynucleotide sequences with **Y** = **2** and **X** = **1** corresponding to the incorporation of **7** and of the phosphoramidite of **1**,[10] respectively. [b] Complementary DNA: 5′-dAGG GGG GAA AAG AAA A. [c] Complementary RNA: 5′-rAGG GGG GAA AAG AAA A. [d] Melting temperatures obtained from the maxima of the first derivatives of the melting curves (A_{260} vs temperature) recorded in a buffer containing 2.5 mM Na_2HPO_4, 5.0 mM NaH_2PO_4, 100 mM NaCl, 0.1 mM EDTA, pH 7.0 using 1.5 μM concentrations of each strand. Values in brackets show the changes in T_m values per modification compared with the reference strand. [e] Target DNA duplex: 5′-dGGT GAA AAA TTT TCT TTT CCC CCC TGA CC; 3′-dCCA CTT TTT AAA AGA AAA GGG GGG ACT GG. [f] Melting temperatures of the duplex to triplex transition obtained from the maxima of the first derivatives of the melting curves (A_{260} vs temperature) recorded in a buffer containing 10 mM sodium cacodylate, 150 mM NaCl and 10 mM $MgCl_2$, pH = 6.0 using 1.5 μM concentration of the TFO and 1.0 μM concentration of the duplex. [g] No transition detected above 10 °C.

dx.doi.org/10.1021/jo200919y |*J. Org. Chem.* 2011, 76, 6177–6187

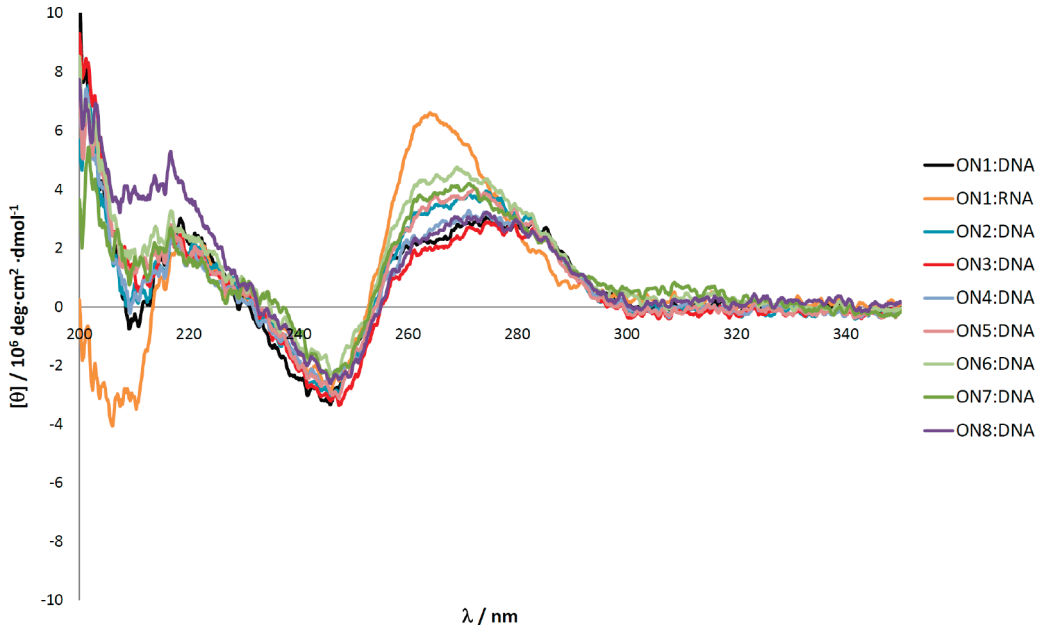

Figure 3. CD spectra of the modified DNA:DNA duplexes.

concerning the duplex stability, and no conclusive differences between **1** and **2** are seen.

When mixed with complementary RNA, the modified oligonucleotides revealed more interesting results. Hence, **ON2** with one incorporation of **1** demonstrated a surprising stabilization of the DNA:RNA duplex (ΔT_m = +1.8 °C), which is contrary to similar single incorporations in the 9-mer sequence (ΔT_m = −2.0 °C),[10] indicating a dependence on the neighboring unmodified nucleosides. This is also demonstrated by the incorporation of the cytidine analogue **2** in **ON3** exhibiting a decrease in T_m (ΔT_m = −2.5 °C). As expected from the former study,[12] consecutive incorporations of stacking phenyl-triazoles by **1** and **2** in **ON4**−**6** markedly increased the melting temperatures with ΔT_m's of 2.0−3.0 °C for each modification, which is fully comparable to the results of 2−3 incorporations of **1** in the shorter 9-mer sequences (ΔT_m = +3.0−4.7 °C).[12] The difference between **ON4** and **ON5** might indicate that a 5′-**XY** motif is slightly better tolerated than a 5′-**YX** motif probably due to different stacking proportions. Four consecutive incorporations of **1** in **ON7** have a significantly more pronounced stabilizing effect than the four consecutive incorporations of **2** in **ON8** (ΔT_m = +3.3 and +1.2 °C per modification, respectively), comparable to the ΔT_m of +5.0 °C observed for each modification with four consecutive incorporations of **1** in a shorter 9-mer sequence.[10]

Finally, we tested the ability of **ON2**−**8** as triplex forming oligonucleotides (TFOs) by mixing these with a 29-mer dsDNA target containing a 16-nucleotide-long stretch of purines known as the HIV-1 polypurine tract.[17] The target DNA duplex has a T_m of 69 °C, and the triplex-to-duplex transition with the unmodified **ON1** was detected at 28 °C. Single incorporations of **1** and **2** led to decreases in melting temperatures of the triplex-to-duplex transition of 1.9 and 4.1 °C in **ON2** and **ON3**, respectively, showing that the 2′-deoxycytidine analogue **2** in the triplex, as well as in the duplexes, is not as well accommodated as the 2′-deoxyuridine analogue **1**. Two consecutive incorporations of **1** and **2** in **ON4**−**5** did not change the picture as destabilizations were observed (ΔT_m = −1.2 and −1.6 °C), but with the three modifications in **ON6**, some stabilization of the triplex was demonstrated (ΔT_m = +0.7 °C). Interestingly, four consecutive incorporations of **1** increased the thermal stability significantly with 7.5 °C (ΔT_m = +1.9 °C/mod), whereas **ON8** with four consecutive incorporations of **2** did not form a detectable triplex. All melting temperatures were determined at pH = 6.0, as no triplex-to-duplex transition was observed above 10 °C in a pH 7.0 buffer for neither the unmodified **ON1** nor any of the modified **ON2**−**8**.

CD Spectroscopy. In order to study structural properties, circular dichroism (CD) spectra were studied for all duplexes and triplexes formed with **ON1**−**8**. It is well-known that different duplex types reveal different CD spectra.[18] Hence, A-type duplexes give an intense negative band at ∼210 nm and a positive band at ∼260 nm, whereas B-type duplexes give a negative band at ∼250 nm and positive bands at ∼220 and ∼280 nm. This can be connected to the fact that DNA:DNA duplexes adopt a B-type form in solution, whereas RNA:RNA duplexes adopt an A-type and DNA:RNA duplexes intermediate A/B-type structures. In Figure 3, the unmodified DNA:DNA duplex formed by **ON1** shows a CD spectrum that is characteristic for a B-type duplex, whereas the corresponding unmodified **ON1**:RNA duplex shows a spectrum for an intermediate A/B duplex type with an increased positive band at ∼260 nm and an increased negative band at ∼210 nm. The modified DNA:DNA duplexes of the present study (Figure 3) demonstrate generally the retention of a B-type duplex with only slightly increased bands at ∼260 nm. However, **ON7** with the four incorporations of **1** demonstrates a more pronounced increase in this band as compared to **ON8** with four incorporations of **2**. This indicates that the uridine analogue has a larger impact on duplex structure than the cytidine analogue. A similar difference can be seen for the single incorporations in **ON2** and **ON3**, showing a larger increase in the 260 nm band for the former. Less clear are the CD spectra of the duplexes formed by **ON4**-**6** with DNA, where **ON4** shows a somewhat smaller change in the CD spectrum as compared to the other two sequences indicating that 5′-**XY** and 5′-**YX** have

dx.doi.org/10.1021/jo200919y |*J. Org. Chem.* 2011, 76, 6177–6187

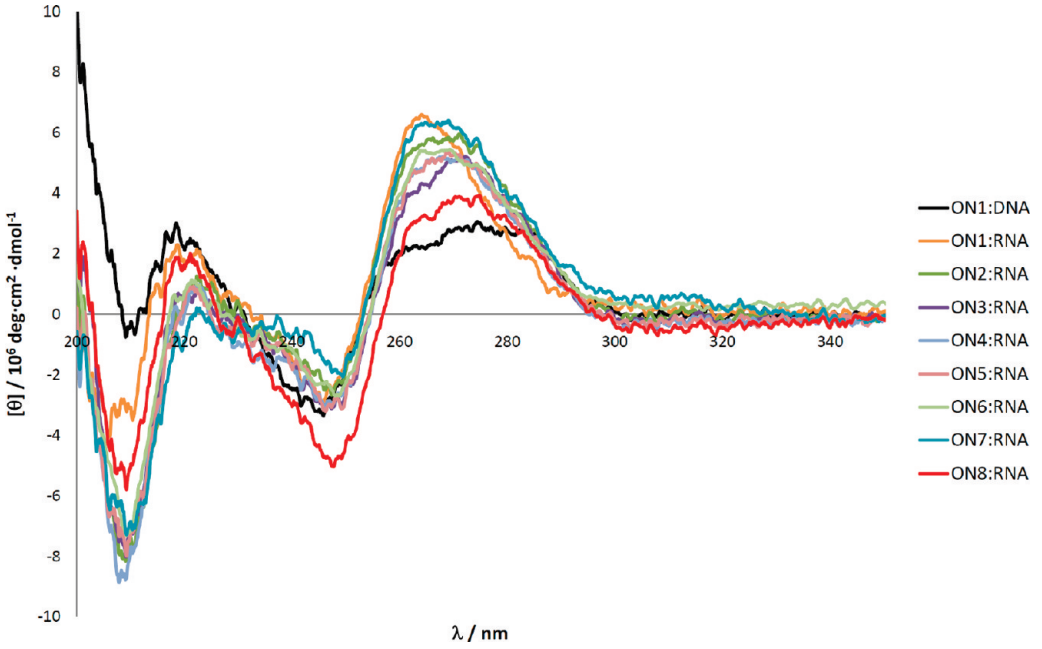

Figure 4. CD spectra of the modified DNA:RNA duplexes.

different impacts on the duplex. Figure 4 shows the CD spectra formed by the modified oligonucleotides **ON2**−**8** with complementary RNA, and all of the duplex spectra are similar to the unmodified DNA:RNA duplex formed by **ON1**. However, especially **ON8** shows some deviation in the form of a much smaller positive band at ∼260 nm and a larger negative band at ∼250 nm. Compared to **ON7**, this indicates again a different change in structure for **2** as compared to **1** in accordance with the thermal stability data (Table 1). CD spectra for the triplexes formed by **ON1**−**8** were also studied, but only small variations were seen and no results leading to conclusions on structural impact were obtained (see Supporting Information for the spectra).

Molecular Modeling. Molecular dynamics simulations were applied to study the DNA:RNA duplexes and the triplexes of the current study. The DNA:RNA hybrid duplexes formed by the oligonucleotides with two and four consecutive incorporations of **1** and **2** (**ON4**−**5** and **ON7**−**8**) as well the two triplexes formed by **ON7**−**8** were built and/or modified within the MacroModel suite of programs[19,20] and studied in a molecular dynamics simulation. The all atom AMBER* force field is modified as described by Pérez et al.[21] and using the GB/SA solvation model as implemented in the AMBER software suite.[22] The initial DNA:RNA hybrid structures were built in the B-type duplex conformation, and the incorporated monomers were subjected to a Monte Carlo conformational search[23] verifying the anti conformation of the torsional angle or the uracil-analogue **1** and the syn conformation of ω for the cytosine-analogue **2** as found via ab initio calcultations (se above, Figures 1 and 2). The obtained lowest energy structure was then subjected to a 5 ns molecular dynamics simulation during which 500 structures were sampled. These 500 structures were subsequently minimized, and the local minimum structure obtained was used for further analysis. Models of the resulting modified duplexes are shown in Figure 5. The four modified DNA:RNA hybrid duplexes were all found to be A/B-type duplexes with the substituents pointing into the major groove. In all cases, a significant stacking was observed between both triazoles and phenyl moieties. However, noteworthy differences can be observed reflecting the different preferred conformations of the torsional angle ω for the two monomers as seen in Figures 1 and 2. The top view of the **ON4**:RNA duplex looking from the 5′-end of the modified sequence shows the cytosine monomer **2** clearly positioned on the top of the uracil monomer **1**, and in the **ON5**:RNA duplex the situation is opposite (Figure 5a and b). The stacking between the two monomers, however, is clearly different due to the phenyl group of **2** pointing away from the duplex and the phenyl group of **1** positioned toward the core of the duplex. The total overlap between the two triazole-phenyl substituents seems somewhat larger in the case of the 5′-**YX** sequence in the **ON4**:RNA duplex than with the 5′-**XY** sequence in the **ON5**:RNA duplex. This observation seems in contrast to the thermal stability of the two duplexes with the latter being slightly more stable (Table 1). However, the relation between stacking energy and aromatic overlap is not direct, and the difference in T_m between the two duplexes is after all only 2 °C. It is also noted that the internal overlap of the two triazole rings alone seems larger in the **ON5**:RNA duplex. The differences are more clear between the two duplexes with four incorporations of either **1** or **2**, i.e., the **ON7**:RNA and the **ON8**.RNA duplexes, respectively (Figure 5c and d). In both cases a perfect stacking orientation of the aromatic moieties were observed, but from the top-views of the two duplexes, the different orientation of the two monomers can be seen. The phenyl group of **2** is again pointing out into the major groove, whereas the phenyl group of **1** is pointing into the duplex core aligning with the nucleobases (as seen in our former study of this monomer in shorter sequences).[10,12] This gives a much larger overlap and subsequent stacking of the phenyl rings with the four consecutive **1** monomers than with the four **2** monomers. This result is in line with the thermal denaturation data on **ON7** showing a significantly stronger duplex with the RNA complement than **ON8** (Table 1).

The models of the two modified triplex structures formed by **ON7** and **ON8** are shown in Figure 6.[20] In the first triplex, the four monomers **1** in **ON7** are clearly showing a coplanar stacking

dx.doi.org/10.1021/jo200919y |*J. Org. Chem.* 2011, 76, 6177–6187

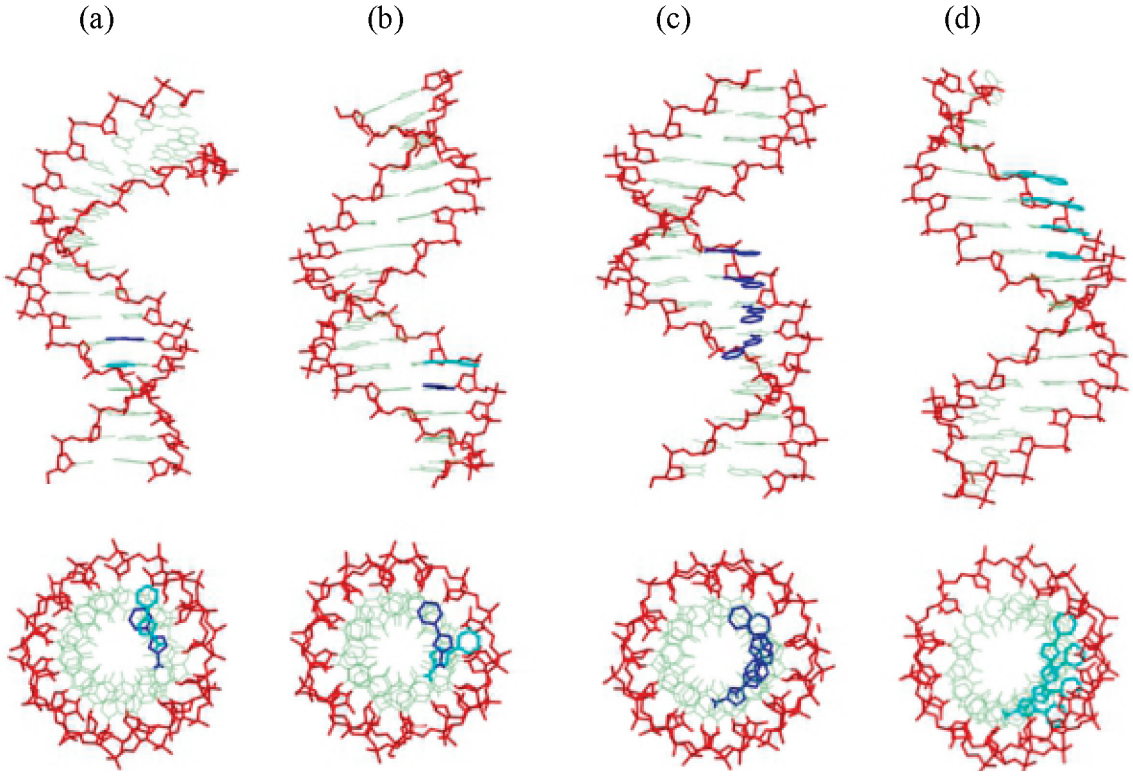

Figure 5. Modeling structures of modified DNA:RNA duplexes. (a) **ON4**:RNA, (b) **ON5**:RNA, (c) **ON7**:RNA, and (d) **ON8**:RNA. Blue = 5-substituents of monomer **X** (**1**); cyan = 5-substituents of monomer **Y** (**2**); red = backbone; green = nucleobases.

orientation of the phenyl-triazole substituents with the torsional angle ω in the expected anti conformation around 180° (Figure 6a). In the top view, the stacking of the substituents involving both the triazoles and the phenyls is clearly seen. In the other triplex formed by **ON8**, the monomers **2** do not show a perfect coplanarity of the aromatic and heteroaromatic rings, and the stacking between the substituents are somewhat hampered (Figure 6b). From the top view it is clear that the phenyl groups are pointing away from the triplex core and not participating in stacking. This might explain the significant difference in stability, where the triplex formed by **ON8** is not stable and the triplex formed by **ON7** is significantly stabilized as compared to the unmodified triplex.

Nuclease Resistance. In order to establish the stability of the modified oligonucleotides against nucleolytic degradation, the modified oligonucleotides were radiolabeled with ^{32}P and mixed with a 3′-exonuclease as well as with fetal calf serum, and the degradation was studied by gel electrophoresis (Figure 7 and 8). **ON1**−**8** were radiolabeled on the 5′-end and digested with snake venom phosphordiesterase (SVPD). Samples were taken after 1, 5, 15, and 30 min and after 1, 4, 16, 24, and 66 h and resolved on denaturing (7 M urea) acrylamide gels (Figure 7). Smaller radioactive fragments migrate faster and are located at the bottom of the gels. As evident from Figure 7, the unmodified **ON1** is degraded within 15 min, whereas all modified oligonucleotides demonstrate a significant resistance toward SVPD. For the single modified **ON2** and **ON3**, SVPD stalls at position 9 and 10 (from the 5′-end), respectively, after removal of the 3′-ends of the sequences. However, the oligonucleotides were completely broken down by 24 h. For the sequences with 2−3 consecutive incorporations of **1** and **2**, **ON4**−**6**, the 3′-ends were again rapidly removed, but SVPD cannot digest past the first modified positions (position 5 or 6) and stalls indefinitely. Hence, two consecutive incorporations are much more efficient than one in protecting the oligonucleotide against the 3′-exonucleoase. In a similar way, the oligonucleotides with four incorporations of **1** or **2**, **ON7**−**8**, demonstrate a rapid digestion of the 3′-end that stops at the first (or second) modification. This design too appears to be stable against SVPD, although completely degraded products appear to increase over 24 h.

The digestion in fetal calf serum was also studied, and as evident from Figure 8 this was faster for the modified oligonucleotides than the 3′-exonucleolytic degradation by SVPD. As all oligonucleotides disappeared after 8 h, probably due to a phosphatase activity removing the ^{32}P-labels, we focused on the reaction in the first 3 h, where a significant stabilization by the modified nucleotides was detected. Whereas the single modified oligonucleotides **ON2**−**3** were almost fully degraded in 3 h, the oligonucleotides with 2−4 consecutive modifications were much more stable, demonstrating a rapid digestion of the 3′-end but then a stall at the first (or second) modification.

DISCUSSION

With the present introduction of the phenyl-triazole substituted cytidine monomer **2** as a supplement to the corresponding uridine monomer **1**, a much wider range of RNA sequences can be targeted. Our hybridization data proves that both monomers can lead to increased thermal stability of the DNA:RNA duplexes if at least two consecutive incorporations are used. This means that from a situation with just **1** in hand, where only RNA sequences with AA stretches are potential targets, we have now broadened the potential to target RNA sequences with just any of

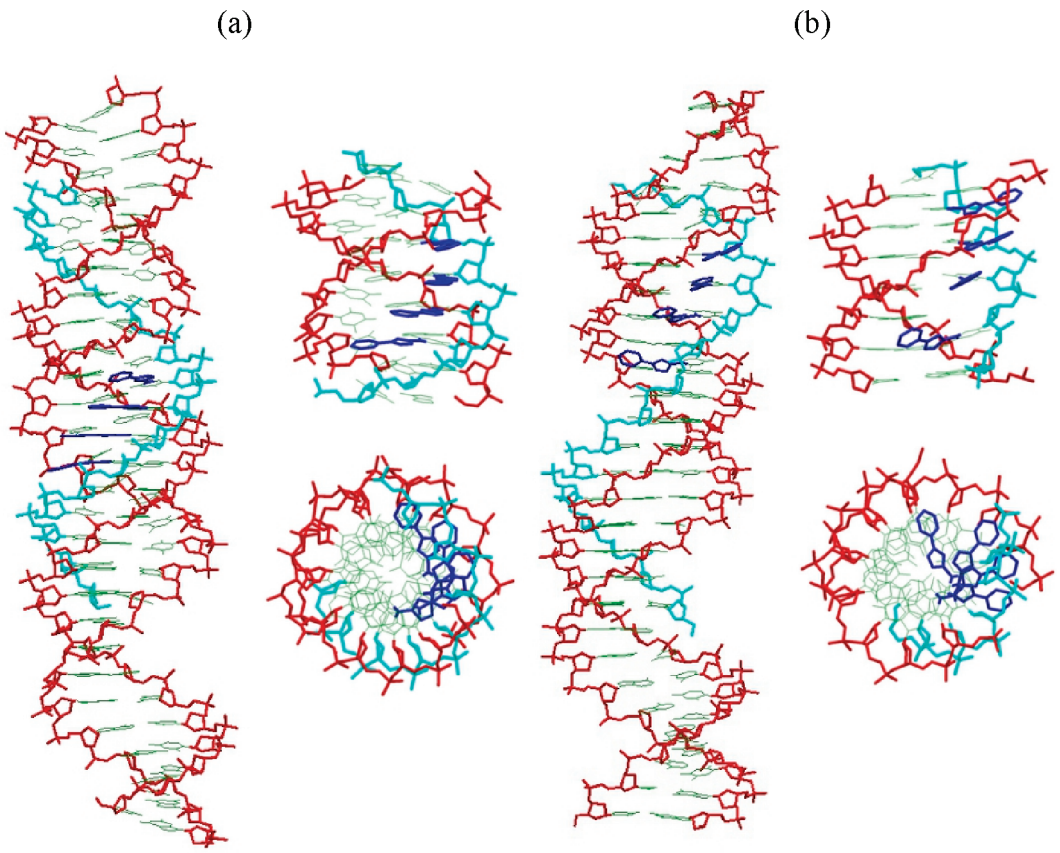

Figure 6. Modeling structures of modified triplexes. (a) **ON7**:dsDNA and (b) **ON8**:dsDNA; full structures, and modified sections in side view and top view. Cyan = backbone of the TFO; blue = 5-substituents of the TFO; red = backbone of the dsDNA; green = nucleobases.

the four possible dipurine stretches. It is clear that the impact on thermal stability is larger with an increasing number of consecutive incorporations and better with consecutive incorporations of the uridine monomer **1** as compared to the cytidine monomer **2**. Nevertheless, a positive impact is found for both monomers. Convincing mis-match discrimination has also been demonstrated for sequences containing consecutive incorporations of **1**.[10] The combination of **1** and **2** hereby allows for a new and very simple approach for the development of potential antisense oligonucleotides. In this aspect, it is very important that the modifications also lead to a very significant stabilization toward nucleolytic degradation, as has been previously observed also for other 5-modified pyrimidine analogues.[24] It adds to this importance that the stabilization increases with two consecutive modifications of **1** or **2**. For the development of antisense oligonucleotides, **1** and **2** can easily be combined with other modifications such as LNA and phosphorthioates that in combination has proven very promising in antisense research.[6] LNA monomers induce a larger increase in thermal stability of DNA:RNA duplexes than the nucleobase substituents of **1** and **2**, but the two kinds of modifications show opposite behavior, as the impact of an LNA monomer is largest by one incorporation and then decreasing, relatively, by the number of consecutive incorporations. Thus, the right balance in affinity needed for securing a selective binding of the target sequences can be programmed with the combination of different modifications such as **1** and **2**. It is therefore also important that the phosphoramidites of both monomers **1** and **2** are easily synthesized with the convenient in situ azidation/CuAAC reaction as the key step.

In contrary to the RNA binding and thereby antisense potential, the triplex-forming and thereby antigene-potential of **1** and **2** is less pronounced. Even though some increase in thermal stability of the triplex can be observed with 3−4 consecutive incorporations, the increase is relatively small and possible only with four incorporations of **1** and not with **2**. Furthermore, the increase obtained with **1** is probably too small as compared to other modifications, for instance, LNA,[17] not the least taking into account that triplexes are in the starting point not very stable as compared to duplexes.

Modeling and CD spectra show that there is a close connection between the structural impact of monomers **1** and **2** on duplexes and the thermal stability. Modeling shows that stacking between monomers, as expected, is the key to the increase in duplex stability. The CD spectra show that the duplexes with the most pronounced relative increases in thermal stability, due to stacking, are also those with most impact on duplex structures. In line with the ab initio calculations proving coplanar but opposite conformations for **1** and **2**, Figure 5 shows that the positioning of the substituents in the duplex is also very different between the two monomers. This has a very clear connection to the stacking of consecutive incorporations of either **1** or **2** (as in **ON7** and **ON8**), but when the two modifications are mixed the difference decreases, and positive influence of stacking exists in both the 5′-**XY** as in the 5′-**YX** sequences. The modeling also demonstrates why the triplex is not stable with four incorporations of **2**, whereas a stabilized triplex is formed with four incorporations of **1**. Hence, there is apparently not room for a sufficient stacking of the phenyls of **2** in the sterically crowded core of the triplex structure.

dx.doi.org/10.1021/jo200919y |*J. Org. Chem.* 2011, 76, 6177–6187

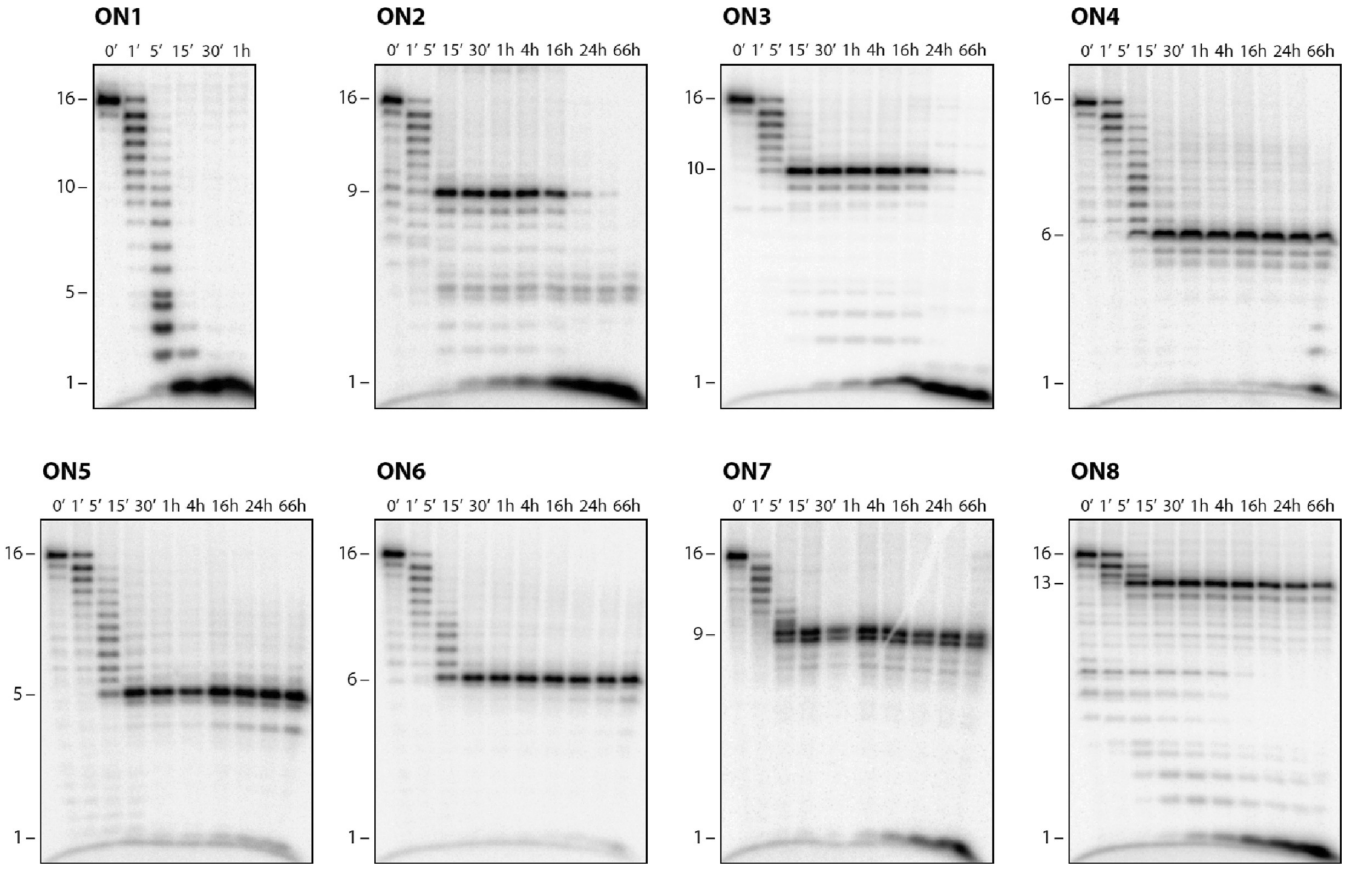

Figure 7. Gel electrophoresis of 5′-^{32}P-labeled oligonucleotides digested by SVPD.

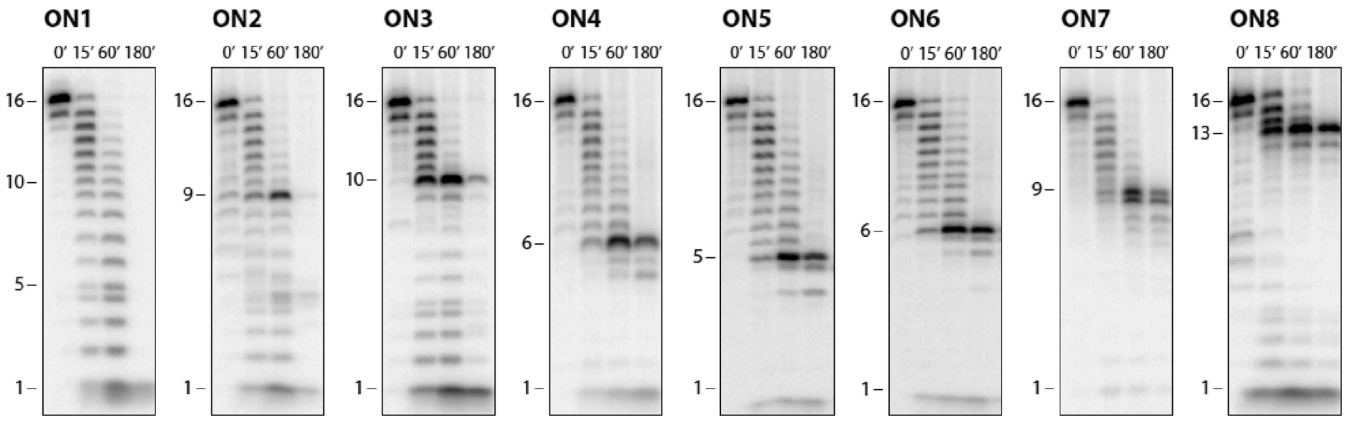

Figure 8. Gel electrophoresis of 5′-^{32}P-labeled oligonucleotides incubated with fetal calf serum.

In addition to the obvious therapeutic potential of **1** and **2** in the antisense approach, the programming of duplex stability by stacking phenyl-triazole substituents in the major groove might also find applications in the preparation of nanomaterials. The delicate correspondence between the substituents, their interdependent stacking and the subsequent influence on structure gives a new possibility in a design where both structure and thermal stability can be controlled. Furthermore, **1** and **2** can be combined with other pyrimidine nucleotide building blocks, on which the CuAAC reaction has been used to attach functional or fluorescent moieties to the 5-position through a triazole, for instance, pyrenes.[25] Hereby, the decrease in duplex stability due to a single triazole modification might be converted to an increase by flanking this modification with **1** and/or **2**.

CONCLUSION

Even though LNA and a few other nucleic acid analogues have set the standard for potential antisense therapeutics, there is still a need for new simple and easily obtained analogues that can be used alone or in combination with other modifications. We believe that the building blocks of the current study, **1** and **2**,

dx.doi.org/10.1021/jo200919y |*J. Org. Chem.* 2011, 76, 6177–6187

together forms such a candidate with the simple synthesis, the increase in RNA recognition due to stacking interactions of phenyl-triazole substituents in the major groove, the programmable RNA-affinity by the combination of the U and C-building blocks, and the high physiological stability.

EXPERIMENTAL SECTION

General. All commercial reagents were used as supplied. Reactions were performed under an atmosphere of nitrogen when anhydrous solvents were used. Column chromatography was carried out on glass columns using silica gel 60 (0.040−0.063 mm). NMR spectra were recorded at 300 or 400 MHz for ^{1}H NMR, at 75 or 100 MHz for ^{13}C NMR, and at 162 MHz for ^{31}P NMR. The δ values are in ppm relative to tetramethylsilane as internal standard or 85% H_3PO_4 as external standard. Assignments of NMR signals are based on 2D spectra and follow the standard nucleoside convention. HR ESI mass spectra were recorded in positive-ion mode.

Preparation of 5-Ethynyl-2′-deoxycytidine (4). A solution of 5-iodo-2′-deoxycytidine, **3**, (1.97 g, 5.58 mmol) in anhydrous DMF (37 mL) and anhydrous triethylamine (19 mL) was degassed and stirred at room temperature. Trimethylsilylacetylene (4.4 g, 44.6 mmol), Pd(PPh_3)$_2Cl_2$ (392 mg, 0.558 mmol) and CuI (106 mg, 0.558 mmol) were added, and the mixture was stirred for 1 h. The mixture was concentrated under reduced pressure, and the residue was co-evaporated with xylene (2 × 30 mL) and purified by flash column chromatography (0−20% MeOH in CH_2Cl_2) to afford the crude TMS-protected intermediate (2.39 g) as a white foam. R_f 0.3 (20% MeOH in CH_2Cl_2). ^{1}H NMR (400 MHz, DMSO-d_6) δ 8.20 (s, 1H, H-6), 7.78 (br s, 1H, NH), 6.60 (br s, 1H, NH), 6.09 (t, J = 6.5 Hz, H-1′), 5.20 (d, J = 4.3 Hz, 1H, 3′-OH), 5.06 (t, Hz, 1H, 5′-OH), 4.20 (m, 1H, H-3′), 3.78 (m, 1H, H-4′), 3.58 (m, 2H, H-5′), 2.14 (ddd, J = 13.1, 5.8, 3.7 Hz, 1H, H-2′), 1.99 (dt, J = 13.2, 6.5 Hz, 1H, H-2′), 0.21 (s, 9H, TMS). ^{13}C NMR (101 MHz, DMSO-d_6) δ 164.09, 153.44, 145.47 (C-6), 99.84, 97.12, 87.65 (C-4′), 85.62 (C-1′), 70.17 (C-3′), 61.16 (C-5′), 40.98 (C-2′), 0.11 ((CH_3)$_3$Si). HR-ESI-MS: m/z 346.1180 [M + Na]$^+$ calcd $C_{14}H_{21}N_3O_4Si\cdot Na^+$ 346.1194. The crude intermediate was dissolved in an 24% aqueous solution of ammonia (40 mL), and the mixture was stirred at room temperature for 2 h. The mixture was concentrated under reduced pressure, and the residue was co-evaporated with 99% ethanol (50 mL) and purified by flash column chromatography (0−30% MeOH in CH_2Cl_2) affording the target nucleoside **4** (1.33 g, 95%) as a white solid. R_f 0.2 (20% MeOH in CH_2Cl_2). ^{1}H NMR (200 MHz, DMSO-d_6) δ 8.25 (s, 1H, H-6′), 7.69 (s, 1H, NH), 6.81 (s, 1H, NH), 6.09 (t, J = 6.4 Hz, 1H, H-1′), 5.21 (d, J = 2.8 Hz, 1H, 3′-OH), 5.09 (t, J = 4.4 Hz, 1H, 5′-OH), 4.33 (s, HC≡C, 1H), 4.20 (m, 1H, H-3′), 3.79 (q, J = 3.2 Hz, 1H, H-4′), 3.65 − 3.51 (m, 2H, H-5′), 2.16 (m, 1H, H-2′), 1.99 (m, 1H, H-2′). ^{13}C NMR (100 MHz DMSO-d_6) δ 164.2, 153.4, 145.4, 88.8, 87.5, 85.8, 85.4, 75.9, 70.0, 60.9, 40.9. HR-ESI-MS: m/z 274.0790 [M + Na]$^+$ calcd $C_{11}H_{13}N_3O_4\cdot Na^+$ 274.0799.

Preparation of 5-(Phenyl-1*H*-1,2,3-triazol-4-yl)-2′-deoxycytidine (2). A mixture of bromobenzene (316 μL, 3.0 mmol), NaN_3 (195 mg, 3.0 mmol), CuI (57 mg, 0.3 mmol), and *N*,*N*′-dimethylethylenediamine (49 μL, 0.45 mmol) in EtOH/H_2O (7:3, v/v, 6 mL) was stirred under microwave irradiation at 100 °C for 1 h and then filtered through a 45 μm filter. Nucleoside **4** (300 mg, 1.19 mmol), TBTA (127 mg, 0.24 mmol), and CuI (34 mg, 0.18 mmol) were added, and the reaction mixture was stirred at room temperature for 96 h and then at 50 °C for 22 h. The mixture was concentrated under reduced pressure, and the residue was purified by flash column chromatography (0−20% MeOH in CH_2Cl_2) affording the product **2** as a white solid (356 mg, 80%). R_f 0.3 (20% MeOH in CH_2Cl_2). ^{1}H NMR (400 MHz, DMSO-d_6) δ 8.86 (s, 1H, H-6), 8.49 (s, 1H, triazole CH), 7.94−7.51 (m, 7H, Ph, NH_2), 6.20 (t, 1H, J = 6.4 Hz, H-1′), 5.25 (d, 1H, J = 4.4 Hz, 3′-OH), 5.19 (t, 1H, J = 4.8 Hz, 5′-OH), 4.27 (m, 1H, H-3′), 3.83 (q, 1H, J = 3.6 Hz, H-4′), 3.72−3.58 (m, 2H, H-5′), 2.23 (m, 1H, H-2′), 2.12 (m, 1H, H-2′). ^{13}C NMR (100 MHz, DMSO-d_6) δ 162.4, 153.8, 142.6, 140.4, 136.4, 129.9, 129.1, 120.4, 119.4, 96.4, 87.3, 85.4, 69.7, 60.8, 40.7. HR-ESI. m/z 393.1290 [M − Na]$^+$ calcd $C_{17}H_{18}N_6O_4\cdot Na^+$ 393.1282.

Preparation of 4-*N*-Acetyl-5-(phenyl-1*H*-1,2,3-triazol-4-yl)-2′-deoxycytidine (5). The nucleoside **2** (442 mg, 1.19 mmol) was co-evaporated with pyridine (2 × 10 mL) and redissolved in the same solvent (12 mL). The solution was stirred at 0 °C, and acetic anhydride (371 μL, 3.39 mmol) was added. The mixture was stirred for 4 h at 0 °C, diluted with CH_2Cl_2 (10 mL) and washed with a saturated aqueous solution of $NaHCO_3$ (10 mL). The aqueous phase was extracted with CH_2Cl_2 (5 × 20 mL), and the combined organic phase was dried ($MgSO_4$) and concentrated under reduced pressure. The residue was purified by flash column chromatography (0−10% MeOH in CH_2Cl_2) to give the peracetylated intermediate as a white solid (355 mg, 60%). R_f 0.9 (10% MeOH in CH_2Cl_2). ^{1}H NMR (400 MHz, DMSO-d_6) δ 10.85 (s, 1H, NH), 9.17 (s, 1H, H-6), 8.42 (s, 1H, triazole CH), 7.94 (m, 2H, Ph), 7.67 (m, 2H, Ph), 7.56 (m, 1H, Ph), 6.19 (t, 1H, J = 6.8 Hz, H-1′), 5.25 (m, 1H, H-3′), 4.39−4.32 (m, 3H, H-4′, H-5′), 2.61−2.48 (m, 2H, H-2′), 2.44 (s, 3H, CH_3CO), 2.10 (s, 3H, CH_3CO), 1.97 (s, 3H, CH_3CO). ^{13}C NMR (100 MHz, DMSO-d_6) δ 170.9, 170.2, 169.96, 158.4, 152.6, 142.6, 141.6, 136.2, 130.0), 129.2, 120.2, 98.7, 87.3, 82.4, 74.1, 63.5, 37.2, 25.9, 20.7, 20.4. HR-ESI: m/z 519.1594 [M − Na]$^+$ calcd $C_{23}H_{24}N_6O_7\cdot Na^+$ 519.1599. The intermediate nucleoside (344 mg, 0.69 mmol) was suspended in 1,4-dioxane (15 mL) and H_2O (7.5 mL), and the mixture was stirred at 0 °C. A solution of sodium hydroxide (110 mg, 2.76 mmol) in H_2O (1.4 mL) was added dropwise, and the reaction mixture was stirred for 2 h at 0 °C. A saturated aqueous solution of ammonium chloride (10 mL) was added, and the mixture was concentrated under reduced pressure. The residue was purified by column chromatography (0−20% MeOH in CH_2Cl_2) to give the product **5** as a white solid (224 mg, 78%). R_f 0.2 (10% MeOH in CH_2Cl_2). ^{1}H NMR (400 MHz, DMSO-d_6) δ 8.92 (s, 1H, H-6), 8.45 (s, 1H, triazole CH), 7.93 (d, J = 7.8 Hz, 2H, Ph), 7.65 (t, J = 7.8 Hz, 2H, Ph), 7.54 (t, J = 7.8 Hz, 1H, Ph), 6.25 (m, 1H, H-1′), 6.13 (br s, 1H, OH), 5.25 (t, J = 2.8 Hz, 1H, 5′-OH), 4.08 (d, J = 2.4 Hz, 1H, H-3′), 3.77−3.38 (m, 3H, H-4′, H-5′), 2.42 − 2.28 (m, 2H, H-2′), 2.08 (s, 3H, CH_3CO). ^{13}C NMR (101 MHz, DMSO) δ 170.1, 162.5, 153.77, 142.3, 140.3, 136.4, 130.0, 129.1, 120.5, 119.8, 96.8, 85.5, 84.9, 74.7, 61.2, 37.8, 20.9. HR-ESI: m/z 435.1383 [M − Na]$^+$ calcd $C_{19}H_{20}N_6O_5\cdot Na^+$ 435.1388.

Preparation of 4-*N*-Acetyl-5′-*O*-(4,4′-dimethoxytrityl)-5-(phenyl-1*H*-1,2,3-triazol-4-yl)-2′-deoxycytidine (6). The nucleoside **5** (192 mg, 0.47 mmol) was co-evaporated with anhydrous pyridine (4 × 10 mL) and redissolved in the same solvent (4.7 mL). 4,4′-Dimethoxytrityl chloride (166 mg, 0.49 mmol) was added, and the reaction mixture was stirred at room temperature for 2 h. Methanol (2 mL) was added, and the mixture was diluted with CH_2Cl_2 (20 mL) and washed with a saturated aqueous solution of $NaHCO_3$ (20 mL). The aqueous phase was extracted with CH_2Cl_2 (4 × 20 mL), and the combined organic phase was dried ($MgSO_4$) and concentrated under reduced pressure. The residue was purified by flash column chromatography (0−20% MeOH and 1% TEA in CH_2Cl_2) to give the product **6** as a white solid (225 mg, 67%). R_f 0.5 (10% MeOH in CH_2Cl_2). ^{1}H NMR (400 MHz, DMSO-d_6) δ 8.46 (s, 1H, triazole CH), 8.18 (s, 1H, H-6), 7.93 (br s, 1H, NH), 7.62 (br s, 1H, NH), 7.55−7.46 (m, 5H, Ph, DMT), 7.32 (d, J = 7.6 Hz, 2H, Ph), 7.22−7.06 (m, 7H, Ph, DMT), 6.74 (m, 4H, DMT), 6.27 (m, 1H, H-1′), 5.15 (m, 1H, H-3′), 4.16 (m, 1H, H-4′), 3.62 (s, 3H, OCH_3), 3.61 (s, 3H, OCH_3), 3.39−3.25 (m, 2H, H-5′), 2.48−2.39 (m, 2H, H-2′), 2.03 (s, 3H, CH_3CO). ^{13}C NMR (101 MHz, DMSO-d_6) δ 169.9, 162.7, 158.0, 153.7, 144.5, 141.9, 139.7, 136.1, 135.3, 129.8, 129.5, 128.9, 127.8, 127.6, 126.7, 120.0, 119.6, 113.1, 97.0, 85.9, 85.6, 83.3, 74.4, 63.5, 54.9, 37.7, 20.8. HR-ESI: m/z 737.2694 [M − Na]$^+$ calcd $C_{40}H_{38}N_6O_7\cdot Na^+$ 737.2695.

dx.doi.org/10.1021/jo200919y |*J. Org. Chem.* 2011, 76, 6177–6187

Preparation of 4-*N*-Acetyl-3′-*O*-(*P*-2-cyanoethyl-*N*,*N*-diisopropylaminophosphinyl)-5′-*O*-(4,4′-dimethoxytrityl)-5-(phenyl-1*H*-1,2,3-triazol-4-yl)-2′-deoxycytidine (7). The nucleoside **6** (150 mg, 0.21 mmol) was co-evaporated with anhydrous 1,2-dichlorethane (2 × 4 mL) and redissolved in the same solvent (2.0 mL). Diisopropylammonium tetrazolide (68 mg, 0.4 mmol) and 2-cyanoethyl-*N*,*N*,*N*′,*N*′-tetraisopropylphosphoramidite (157 mg, 0.52 mmol) was added, and the mixture was stirred at room temperature for 25 h. Methanol (2 mL) was added, and the mixture was purified by flash column chromatography (0−10% MeOH and 1% TFA in CH_2Cl_2) to give the product **7** as a white solid (164 mg, 85%). R_f 0.5 (5% MeOH in CH_2Cl_2). ^{31}P NMR (162 MHz, $CDCl_3$) δ 149.61, 149.36, 148.89, 148.48 (rotamers). HR-ESI: m/z 915.3910 $[M - H]^+$ $C_{49}H_{55}N_8O_8P \cdot H^+$ calcd 915.3953.

Oligonucleotide Synthesis. Oligonucleotide synthesis was carried out on an automated DNA synthesizer following the phosphoramidite approach. Synthesis of oligonucleotides **ON2**−**8** was performed on a 0.2 μmol scale (CPG support) by using the modified nucleoside phosphoramidites (**7** and the corresponding amidite of **1**[10]) as well as the corresponding commercial 2-cyanoethyl phosphoramidites of the natural 2′-deoxynucleosides. The synthesis followed the regular protocol for the DNA synthesizer. For the modified phosphoramidites a prolonged coupling time of 20 min was used. 1*H*-Tetrazole was used as activator. Coupling yields for all 2-cyanoethyl phosphoramidites were >96%. The 5′-*O*-DMT-ON oligonucleotides were removed from the solid support by treatment with concentrated aqueous ammonia at 55 °C for 12 h. The oligonucleotides were purified by reversed-phase HPLC on a Waters 600 system using Xterra MS C18 10 μm; 7.8 × 150 mm column + precolumn: Xterra MS C18 10 μm, 7.8 × 10 mm. Buffer A: 0.05 M triethyl ammonium acetate, pH 7.4. Buffer B: 75% MeCN/H_2O (3:1, v/v). Program used: 2 min 100% A, 100−30% A over 38 min, 10 min 100% B, 10 min 100% A. All oligonucleotides were detritylated by treatment with 80% aqueous acetic acid for 20 min and neutralized by addition of sodium acetate (3 M, 15 μL), and then sodium perchlorate (5 M, 15 μL) was added followed by acetone (1 mL). The pure oligonucleotides precipitated overnight at −20 °C. The mixture was then placed in a centrifuge and subjected to 12,000 rpm, 10 min at 4 °C. The supernatant was removed, and the pellet was washed with cold acetone (2 × 1 mL). The pellet was then dried for 30 min under reduced pressure and dissolved in pure water (500 μL), and the concentration was measured as OD at 260 nm. The purity was confirmed by IC analysis. MALDI-TOF MS $[M - H]^-$ gave the following results (calcd/found): **ON2** (4831.2/4830.8), **ON3** (4845.2/4846.3), **ON4** (4974.3/4974.4), **ON5** (4974.3/4974.6), **ON6** (5105.5/5106.4), **ON7** (5218.6/5219.2) and **ON8** (5274.7/5276.3).

Thermal Denaturation Experiments. Extinction coefficients of the modified oligonucleotides were estimated from a standard method but calibrated by the micromolar extinction coefficients of the monomeric compounds **1** and **2**, which were estimated from their UV spectra (**1**, ε_{260} = 7.8;[10] **2**, ε_{260} = 13.5). UV melting experiments were thereafter carried out on a UV spectrometer. For the duplex studies, samples were dissolved in a medium salt buffer containing 2.5 mM Na_2HPO_4, 5 mM NaH_2PO_4, 100 mM NaCl, and 0.1 mM EDTA at pH = 7.0 with 1.5 μM concentrations of the two complementary oligonucleotide sequences. The increase in absorbance at 260 nm as a function of time was recorded while the temperature was increased linearly from 5 to 80 or 90 °C at a rate of 1.0 °C/min by means of a Peltier temperature programmer. For the triplex studies, heating was performed at a rate of 0.5 °C/min in a buffer containing 10 mM sodium cacodylate, 150 mM NaCl and 10 mM $MgCl_2$, pH = 6.0. The melting temperature was determined as the local maximum of the first derivatives of the absorbance vs temperature curve. The melting curves were found to be reversible. All determinations are averages of at least duplicates within ±0.5 °C.

Circular Dichroism Spectroscopy. CD spectra were obtained at 5 °C using the same medium salt buffer as in the UV melting experiments with 1.5 μM concentrations of the two complementary oligonucleotide sequences.

Molecular Modeling. *General Parameters.* In all of the calculations the phosphodiester backbone charge was neutralized with sodium ions, placed 3.0 Å from the negatively charged oxygen atoms in the plane described by the phosphorus and the nonbridging oxygen atoms. The sodium ions were constrained throughout the series of calculations by a force constant of 418 KJ/molÅ^2. The AMBER* force field supplied with MacroModel V9.1,[19] atom type and GB/SA solvation model was adapted and modified using the parambsc0 parameters.[21,22]

Generation of Starting Structure Procedure. A standard B-type DNA:DNA helix I built in the MacroModel V.9.1 suite of programs[19] and modified with the appropriate C-5 thymine modification to form **ON1**−**10**. The model structure was subjected to an torsional rotation MCMM structure search.[23] In the MCMM structure search the rotation around C1′/N1, C5/C1″, and N1′/C1″ bonds are given a 180° rotational freedom, and during the MCMM 1000 structures are generated. The obtained structures are subjected to a multiple minimization to reduce the number of structures generated into a number of local and global minima. The global minima structure generated is then used in the subsequent MD simulation.

Molecular Dynamics Parameters. The global energy structure obtained was subjected to a 5 ns MD simulation (simulation temperature 300 K, time step 2.2 fs, SHAKE all bonds to hydrogen and the molecular dynamics setting) during which 500 individual structures were sampled. These sample structures were subsequently minimized to obtain a converged global minimum. The duplex structures were minimized using the Polak−Ribiere conjugate gradient method, the modified all-atom AMBER force field[19,23,26,27] and modified GB/SA solvation model[22] implemented in MacroModel V9.1. Nonbonded interactions were treated with extended cut-offs (van der Waals 8.0 Å and electrostatics 20.0 Å). The 500 sample structures were subjected to a multiple minimization to identify the global and local minima sampled. The global minimum was used for analysis.

Nuclease Resistance Assays. Oligonucleotide stability against snake venom phosphodiesterase I from *Crotalus adamanteus* (Pharmacia Biotech) was evaluated by incubating 3 μM of of 5′-^{32}P-labeled oligonucleotide with 6.7 ng/μL phosphodiesterase I in 100 mM Tris-HCl (pH 8.0), 15 mM $MgCl_2$, at 21 °C. Initial samples (0 min) were drawn immediately prior to adding the enzyme. Oligonucleotide stability in fetal calf serum (Biochrom AG) was evaluated by incubating 2 μM of 5′-^{32}P-labeled oligonucleotides in a 1:1 mixture of serum and water. Aliquots were quenched with 1 vol ice-cold 95% formamide with excess EDTA. Samples were resolved on 13% denaturing polyacrylamide electrophoresis gels with 7 M urea and visualized by autoradiography.

■ ASSOCIATED CONTENT

Supporting Information. CD spectra for the studied triplexes and selected NMR spectra. This material is available free of charge via the Internet at http://pubs.acs.org.

■ AUTHOR INFORMATION

Corresponding Author
*E-mail: pon@ifk.sdu.dk.

■ ACKNOWLEDGMENT

The project was supported by The Danish Research Agency's Programme for Young Researchers, Nucleic Acid Center and The Danish National Research Foundation, The Danish Council for Independent Research, Technology and Production Sciences (FTP) and Natural Sciences (FNU), Danish Center for Scientific Computing and Møllerens Fond.

REFERENCES

(1) (a) Zamecnik, P. C.; Stephenson, M. L. *Proc. Natl. Acad. Sci. U.S.A.* **1978**, *75*, 280–284. (b) Stephenson, M. L.; Zamecnik, P. C. *Proc. Natl. Acad. Sci. U.S.A.* **1978**, *75*, 285–288.

(2) Uhlmann, E.; Peyman, A. *Chem. Rev.* **1990**, *90*, 543–580.

(3) (a) Kurreck, J. *Eur. J. Biochem.* **2003**, *270*, 1628–1644. (b) Bell, N. M.; Micklefield, J. *ChemBioChem* **2009**, *10*, 2691–2703.

(4) Buchini, S.; Leumann, C. J. *Curr. Opin. Chem. Biol.* **2003**, *7*, 717–726.

(5) (a) Freier, S.; Altmann, K.-H. *Nucleic Acid Res.* **1997**, *25*, 4429–4443. (b) Aboul-Fadl, T. *Curr. Med. Chem.* **2005**, *12*, 2193–2214. (c) Cobb, A. J. A. *Org. Biomol. Chem.* **2007**, *5*, 3260–3275. (d) Lebreton, J.; Escudier, J.-M.; Arzel, L.; Len, C. *Chem. Rev.* **2010**, *110*, 3371–3418.

(6) (a) Vester, B.; Wengel, J. *Biochemistry* **2004**, *43*, 13233–13241. (b) Kaur, H.; Babu, B. R.; Maiti, S. *Chem. Rev.* **2007**, *107*, 4672–4697. (c) Nielsen, P.; Wengel, J. In *Modified Nucleosides in Biochemistry, Biotechnology and Medicine*; Herdewijn, P., Ed.; Wiley-VCH: Weinheim, 2008; pp 133−152.

(7) Luyten, I.; Herdewijn, P. *Eur. J. Med. Chem.* **1998**, *33*, 515–576.

(8) Lin, K.-Y.; Jones, R. J.; Matteucci, M. *J. Am. Chem. Soc.* **1995**, *117*, 3873–3874.

(9) (a) Wagner, R. W.; Matteucci, M. D.; Lewis, J. G.; Gutierrez, A. J.; Moulds, C. M.; Froehler, B. C. *Science* **1993**, *260*, 1510–1513. (b) Gutierrez, A. J.; Matteucci, M. D.; Grant, D.; Matsumura, S.; Wagner, R. W.; Froehler, B. C. *Biochemistry* **1997**, *36*, 743–748. (c) Gutierrez, A. J.; Terhorst, T. J.; Matteucci, M. D.; Froehler, B. C. *J. Am. Chem. Soc.* **1994**, *116*, 5540–5544. (d) Sinkeldam, R. W.; Greco, N. J.; Tor, Y. *ChemBioChem* **2008**, *9*, 706–709.

(10) Kočalka, P.; Andersen, N. K.; Jensen, F.; Nielsen, P. *ChemBioChem* **2007**, *8*, 2106–2116.

(11) (a) Tornøe, C. W.; Christensen, C.; Meldal, M. *J. Org. Chem.* **2002**, *67*, 3057–3064. (b) Rostovtsev, V. V.; Green, L. G.; Fokin, V. V.; Sharpless, K. B. *Angew. Chem., Int. Ed.* **2002**, *41*, 2596–2599.

(12) Andersen, N. K.; Chandak, N.; Brulíková, L.; Kumar, P.; Jensen, M. D.; Jensen, F.; Sharma, P. K.; Nielsen, P. *Bioorg. Med. Chem.* **2010**, *18*, 4702–4710.

(13) A preliminary synthesis of compound **2** has been published in a conference proceeding: Andersen, N. K.; Spáčilová, L.; Jensen, M. D.; Kočalka, P.; Jensen, F.; Nielsen, P. *Nucleic Acids Symp. Ser.* **2008**, *52*, 149–150.

(14) Independently, compound **2** has been recently presented as a fluorescent nucleoside analogue: Dodd, D. W.; Swanick, K. N.; Price, J. T.; Brazeau, A. L.; Ferguson, M. J.; Jones, N. D.; Hudson, R. H. E. *Org. Biomol. Chem.* **2010**, *8*, 663–666.

(15) Frisch, M. J. et al. ; *Gaussian 03*; Gaussian Inc.: Wallingford, CT, 2004

(16) (a) Barr, P. J.; Jones, A. S.; Serafinowski, P.; Walker, R. T. *J. Chem. Soc., Perkin Trans. 1* **1978**, 1263–1267. (b) Marsh, A.; Alcock, N. W.; Errington, W.; Sagar, R. *Tetrahedron* **2003**, *59*, 5595–5601.

(17) Højland, T.; Kumar, S.; Babu, B. R.; Umemoto, T.; Albæk, N.; Sharma, P. K.; Nielsen, P.; Wengel, J. *Org. Biomol. Chem.* **2007**, *5*, 2375–2379.

(18) Saenger, W. *Principles of Nucleic Acid Structure*; Springer: New York, 1984.

(19) *MacroModel*, version 9.1; Schrödinger, LLC: New York, NY, 2005.

(20) The triplex structure was built via the web page http://w3dna.rutgers.edu/ allowing full control of sequence design, and the generated structure was exported as a pdb file and modified accordingly.

(21) Pérez, A.; Marchán, I.; Svozil, D.; Sponer, J.; Cheatham, T. E.; Laughton, C. A.; Orozco, M. *Biophys. J.* **2007**, *92*, 3817–3829.

(22) Still, W. C.; Tempczyk, A.; Hawley, R. C.; Hendrickson, T. *J. Am. Chem. Soc.* **1990**, *112*, 6127–6129.

(23) Chang, G.; Guida, W. C.; Still, W. C. *J. Am. Chem. Soc.* **1989**, *111*, 4379–4386.

(24) Østergaard, M. E.; Kumar, P.; Baral, B.; Raible, D. J.; Kumar, T. S.; Anderson, B. A.; Guenther, D. C.; Deobald, L.; Paszczynski, A. J.; Sharma, P. K.; Hrdlicka, P. J. *ChemBioChem* **2009**, *10*, 2740–2743.

(25) Østergaard, M. E.; Guenther, D. C.; Kumar, P.; Baral, B.; Deobald, L.; Paszczynski, A. J.; Sharma, P. K.; Hrdlicka, P. J. *Chem. Commun.* **2010**, *46*, 4929–4931.

(26) Weiner, S. J.; Kollman, P. A.; Case, D. A.; Singh, U. C.; Ghio, C.; Alagona, G.; Profeta, S.; Weiner, P. *J. Am. Chem. Soc.* **1984**, *106*, 765–784.

(27) Weiner, S. J.; Kollman, P. A.; Nguyen, D. T.; Case, D. A. *J. Comput. Chem.* **1986**, *7*, 230–252.